ELSEVIER

Thermochimica Acta 396 (2003) 109–117

thermochimica acta

www.elsevier.com/locate/tca

Frequency dependence of the heat capacity of polystyrene in the glass transition region measured by multi-frequency light-modulated DSC☆

P. Kamasa[a,b,1], M. Pyda[a,b], A. Buzin[a,b], B. Wunderlich[a,b,*]

[a] *Department of Chemistry, University of Tennessee, Knoxville, TN 37996-1600, USA*
[b] *Oak Ridge National Laboratory, Chemical and Analytical Science Division, Oak Ridge, TN 37831-6197, USA*

Received 29 November 2001; received in revised form 30 June 2002; accepted 2 October 2002

Abstract

The reversing heat capacity of polystyrene has been measured in the glass transition region as a function of frequency by temperature-modulated DSC using infra-red light for the modulation. The mean temperature was controlled by the calorimeter operating in the standard DSC mode. The additional power transferred to the specimens is obtained by infra-red diodes with their mean power controlled by a pulse-width modulation method. This method allows to synthesize sinusoidal temperature-profiles with negligible distortion with frequencies of up to 0.125 Hz. The experiments were carried out using multi-frequency temperature-profiles composed by superposition of four sinusoidal modulations of periods of 243, 81, 27, and 9 s, which cover the frequency range from the 1st to the 27th harmonic. To study the kinetics in the glass transition region, the thermal history was produced by cooling the samples at different rates. The results and the advantages of the new method are discussed and compared to a series of less-precise separate single-frequency analyses.

Keywords: TMDSC; DSC; LMDSC; Temperature modulation by infra-red light; Glass transition; Frequency-dependent heat capacity; Polystyrene

1. Introduction

Glasses are meta-stable and undergo a characteristic, time-dependent transformation on heating when changing to the liquid state at their glass transition temperature, T_g. Depending on the thermal history, glasses have different thermodynamic properties, measurable by their enthalpy, H, and Gibbs function, G. Both are linked to the heat capacity, $C_p = \partial H/\partial T$ and $C_p = -T(\partial^2 G/\partial T^2)$, and are measurable by calorimetry. There are a number of calorimetric techniques, of which the standard differential scanning calorimetry (DSC) has gained increasing popularity over the years. The standard DSC which employs a linear heating rate for scanning, however, leads to complications in the glass transition region. Different DSC traces are observed on heating of glasses with different histories at the same heating rate, or on

☆ The submitted manuscript has been authored by a contractor of the US Government under the contract No. DOE-AC05-00OR22725. Accordingly, the US Government retains a non-exclusive, royalty-free license to publish or reproduce the published form of this contribution, or allow others to do so, for US Government purposes.

* Corresponding author. Present address: Department of Chemistry, University of Tennessee, Knoxville, TN 37996-1600, USA. *E-mail address:* wunderlich@chartertn.net (B. Wunderlich).

[1] On leave from the Research Institute for Solid State Physics and Optics, Hungarian Academy of Science, Budapest.

0040-6031/02/$ – see front matter
PII: S0040-6031(02)00527-0

heating a glass with a given thermal history with different heating rates. A first approximate description of such behavior was linked to the hole model of the glass transition and described, using a simple, first-order kinetics expression [1]. With the invention and development of temperature-modulated differential scanning calorimetry (TMDSC) [2], the frequency-dependence of the heat capacity could be measured directly and similarly analyzed [3–8]. A pseudo-isothermal analysis at different frequencies and amplitudes of temperature modulation of the glass transition of polystyrene was carried out and described as a relaxation process [6]. A number of other modulation techniques have been developed since the introduction of TMDSC. Of special interest is the multi-frequency modulation with a complex sawtooth [9] which permits the measurement of an apparent heat capacity as a function of frequency in a single experiment. This method with complex sawtooth modulation has been used to measure the frequency dependence of the heat capacity in the glass transition region of polystyrene [10]. This first experiment with a complex sawtooth indicated the need for data with higher frequencies than possible using the standard temperature control of a heat-flux DSC. Beside the use of conventional heaters, radiant energy as a heating source has been used to modulate the temperature, called light-modulation calorimetry [11,12]. In comparison with conventional heaters, the light-modulation applied to standard DSC (LMDSC) has the advantage of a wider choice of operating frequencies.

In the present work, both, multi-frequency sawtooth modulation and the use of radiant energy have been combined to find the apparent, reversing heat capacity of polystyrene as a function of frequency in the glass transition region.

2. Experimental details and results

2.1. DSC equipment and samples

A commercial Thermal Analyst 2910® system from TA Instrument in the standard DSC mode was used for all measurements. The temperature of the sample and reference is regulated by the original temperature controller in its standard mode. The sinusoidal modulation software and corresponding evaluation as provided by the manufacturer where not used in the present experiments. The temperature was calibrated in the usual manner with the melting temperatures of indium and water at heating rates of $10\,\mathrm{K\,min^{-1}}$. The heat-flow rate Φ, as measured by the temperature difference $\Delta T = T_\mathrm{r} - T_\mathrm{s}$, was initially set by the heat of fusion of indium, and then corrected with calibration runs with Al_2O_3 in form of a sapphire single crystal. Dry nitrogen gas with a flow rate of $15\,\mathrm{ml\,min^{-1}}$ was purged though the DSC cell. No additional cooling was necessary in the temperature range of interest.

The polystyrene used was purchased from Aldrich Chemical Co. Its glass transition temperature is about 373 K under standard analysis conditions of heating at $10\,\mathrm{K\,min^{-1}}$, and the mass-average molar mass is equal to 280,000 Da, measured by size-exclusion chromatography by the supplier. The same sample of a weight of about 22 mg was used for all experiments.

2.2. Complex sawtooth modulation

The complex sawtooth modulation mode consists of a series of linear heating and cooling segments, chosen to produced 1st, 3rd, 5th and 7th harmonics with practically equal amplitude, the 9th harmonic of somewhat lower amplitude, and almost negligible higher harmonics. The details of the method and a table of the 14 program steps for the temperature modulation were given previously [9]. The multi-frequency sawtooth modulation in our experiment covers frequencies from 2.38×10^{-3} to 0.021 Hz with corresponding periods of 420, 120, 84, 60, and 46.67 s. The upper frequency limit is determined mainly by a time constant $R_\mathrm{th} \times C_\mathrm{r}$, a product of the thermal resistivity between heater and sample and the heat capacity of the calorimeter. Quasi-isothermal experiments were performed at several base temperatures, T_0, after heating to about 393 K, followed by cooling to 343 K with a rate of $10\,\mathrm{K\,min^{-1}}$.

Due to the thermal resistance between the pan and sample, as well as pan and thermocouple, and the thermal conductivity of the sample, the obtained heat capacity is frequency-dependent, and therefore, appropriate corrections must be done for the calculation of the heat capacity. Using a model of heat conducting between the temperature sensor and the pan, and then the pan and the sample, the correction of the heat capacity determination in a temperature-modulated

DSC was considered in detail by Moon et al. [13], but a suitable equation could not be derived.

Assuming steady state and stationarity, the heat capacity can be calculated from the amplitude of modulated temperature of the sample, A_{Ts}, and the amplitude of the heat-flow rate A_Φ. In the pseudo- as well as quasi-isothermal method of TMDSC an apparent, reversing heat capacity can then be evaluated from the following equation [14]:

$$C_p = \frac{A_\Phi}{A_{Ts}} \frac{1}{\omega} K(\omega) \tag{1}$$

where ω is the angular frequency of the modulation in rad s^{-1}. The correction function $K(\omega)$ was suggested to have the form

$$K(\omega) = \sqrt{1 + \tau_c^2 \omega^2} \tag{2}$$

where τ_c ($=R_{th}C_r$) is a time constant to be calculated from the heat capacity of the empty reference calorimeter (pan), C_r, and the Newton's law of thermal resistance. It was found that better accuracy can be obtained by evaluation of τ_c experimentally [15]. At higher frequency τ_c is a non-linear function of frequency itself.

The procedure of the frequency correction is shown in the four parts of Fig. 1. The heat capacity as measured, without correction, is obtained from the ratio $C_p(\text{meas}) = A_\Phi/(A_{Ts}\omega)$, where $A_{Ts}\omega$ represents the modulation amplitude of the heating rate. To determine the amplitude of the modulated temperature and the heat-flow rate at different frequencies, a Fourier-transform was made and the five harmonics of the complex sawtooth are used in Eqs. (1) and (2). The measured values of heat capacity are depicted in Fig. 1a in the temperature range from below to above the glass transition as a function of the frequency of the harmonics $\nu(= \omega/2\pi)$. The time constant τ_c is obtained from a plot of the inverse of the squared, measured heat capacity versus the square of the frequency [15]:

$$\frac{1}{C_p(\text{meas})^2} = \frac{1}{C_p^2}[1 + \tau_c^2(\omega)^2] \tag{3}$$

as is illustrated in Fig. 1b. From the Fig. 1b one can see that only data outside the region of the glass transition can be approximated by a linear function. This approximation is not valid in the glass transition region. Using the procedure of Eq. (3) within the glass transition region leads to an increase of the standard deviation, S.D., as is illustrated in Fig. 1c. The parameter τ_c in this region is much larger since it now correspond not only to a time constant of the calorimeter, but also contains a contribution of the sample itself. To obtain a heat capacity independent of the time constant of the calorimeter, the value of τ_c of Eq. (2) calculated in the region outside the glass transition, was extrapolated for data inside the glass transition. The frequency-corrected apparent specific heat capacity throughout the glass transition region is then illustrated in Fig. 1d. It can be seen that while the heat capacity below the glass transition is frequency independent, in the glass transition, the heat capacity decreases with frequency. Near the liquid region, the change with frequency is larger. Above the glass transition, the heat capacity is again frequency independent.

The frequency-dependent heat capacity may be fitted to a complex function, characteristic for two or more subsystems, and characterized by a time necessary for the exchange of energy between these subsystems, an enthalpy-relaxation time, τ_{enthalpy}. The approximation for the experimental data at 376 K is drawn as a solid line in Fig. 1d. The relation is obtained by fitting parameters of the real, c_p', and the imaginary part c_p'', as depicted by the dashed lines

$$c_p' = \frac{\Delta c_p}{1 + (\nu\tau_{\text{enthalpy}})^\alpha} \quad \text{and}$$

$$c_p'' = \frac{(\nu\tau_{\text{enthalpy}})^{\alpha/2}\, \Delta c_p}{1 + (\nu\tau_{\text{enthalpy}})^\alpha} \tag{4a}$$

as components of heat capacity

$$c_p = \sqrt{(c_p')^2 + (c_p'')^2} + c_{p,\text{inf}} \tag{4b}$$

depicted by the solid line, where α replaces the square in Eq. (2), $c_{p,\text{inf}}$ is a heat capacity for infinitely high frequency, i.e., the heat capacity of the glass, and Δc_p is the difference between the heat capacity of the liquid and the glass. The best fitting was found for $\tau_{\text{enthalpy}} =$ 35 s and $\alpha = 1.8$, $\Delta c_p = 0.38\,\text{J K}^{-1}\,\text{g}^{-1}$ and $c_{p,\text{inf}} =$ $1.247\,\text{J K}^{-1}\,\text{g}^{-1}$. The data in the frequency domain displayed in Fig. 1d can be easy transformed to the heat capacity as a function of temperature for each frequency, as shown in Fig. 2.

From the above analysis it is seen that to obtain the relaxation time, τ_{enthalpy}, directly from the measured

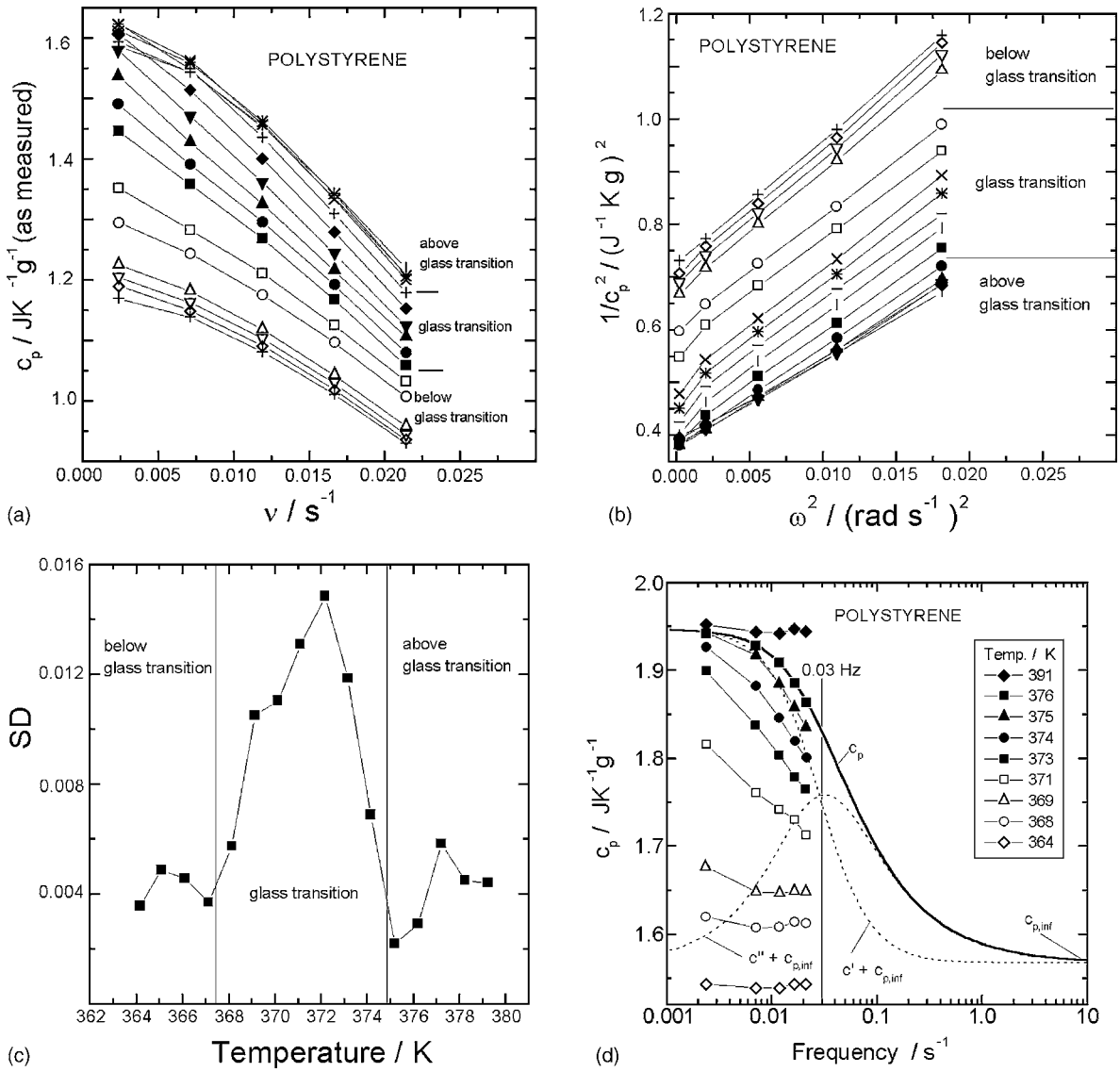

Fig. 1. (a) Uncorrected specific heat capacity in the temperature range from below to above glass transition of polystyrene, obtained using Fourier transformation of the data of modulated sample temperature and heat-flow rate using Eq. (1). (b) Plot of the inverse of the squared, measured specific heat capacity versus the square of the frequency to obtain the time constant τ_c. (c) Values of the standard deviation, S.D., from a linear approximation of the data in Fig. 1b. (d) Frequency-corrected specific heat capacity depicted on the left side by the symbols, and the approximation of the frequency-dependent specific heat capacity c_p at 376 K.

data, it is useful to carry out experiments at higher frequency than 0.03 Hz. The light-modulation experiment can reach a frequency of 0.11 Hz, as indicated in next Figs. 4 and 5 using the same calorimeter as used for the complex sawtooth modulation with modifications, as is described next.

2.3. Light-modulated DSC experiments

As mentioned above, the upper frequency limit is determined by a time constant $R_{th}C_r$, consisting of thermal resistivity between heater and sample, and the heat capacity of the calorimeter. While the heat

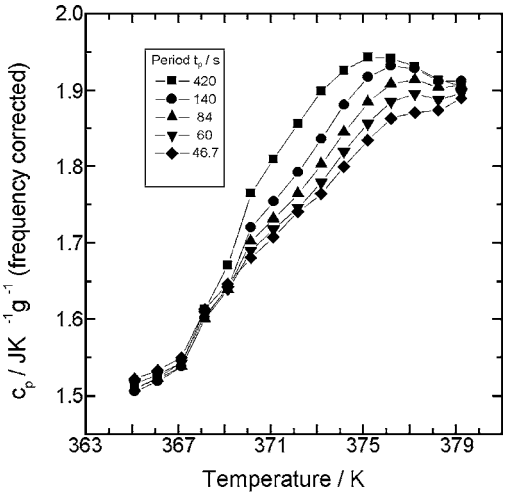

Fig. 2. Frequency-corrected specific heat capacity as a function of temperature for the periods indicated.

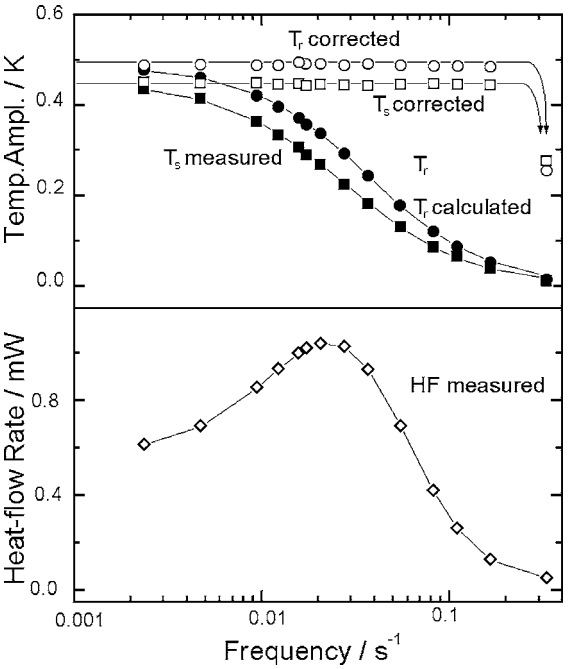

Fig. 3. Principle for the frequency correction, proposed for LMDSC as described in the text and illustrated on the example of Al_2O_3 at 369.5 K.

capacity of the calorimeter cannot be reduced, the thermal resistivity depends on the heating source. An additional radiant energy source near the specimens decreases this resistivity and modulation may by obtained at higher frequencies than possible in the standard mode of operation. The radiant energy is generated by two infrared light emitting diodes with radiant power output, each of 100 mW. Light from a distance of 4 mm is focused at the top of the sample and reference pans. The modification of the calorimeter is described in detail in another publication [16] and consists mainly of replacing the DSC cover with a sapphire disk to admit the radiation. The amount of energy transferred to the specimens is controlled by the pulse-width modulation (PWM) method. The PWM method is known from the early years of development of the information transmission technique (see for instance [17]), but has not routinely been applied to LMDSC.

Measurements using LMDSC were carried out with the same sample and calorimeter as used for the complex sawtooth modulation. Multi- or single-frequency programs were applied consisting of four frequencies with periods of 243, 81, 27, and 9 s. Each subsequent frequency was chosen to be the 3rd harmonic of the prior, lower frequency. Such choice is optimal to obtain a wide frequency range, reaching the 27th harmonic with a minimum of unavoidable losses due to the amplitudes shared between the harmonics in the multi-frequency mode. Two kinds of experiments were carried out with the light-modulation, quasi-isothermal TMDSC at a series of base temperatures, T_0, and standard TMDSC with underlying heating and cooling rates of $\langle q \rangle = 1.0\,\mathrm{K\,min^{-1}}$.

The main feature of the LMDSC using PWM is a linear control which allows the formation of any arbitrary temperature profile with a frequency limit that is determined by a new time constant $\tau_c = R_{th}C_r$ where R_{th} is the thermal resistivity of the sample-diode system. The heat capacity C_r is reduced to a local heat capacity of the surroundings of the sample and reference pans within the area where the temperature is modulated. Because of the wide frequency range covering 27 harmonics, the corrections as used for the sawtooth modulation become insufficient. The problem is illustrated in Fig. 3 on the example of a measurement of the heat capacity of sapphire. The details, again, were described earlier [16]. The amplitude of the modulated temperature, A_{Ts}, and the amplitude of the heat-flow rate response, A_Φ, are obtained using

Fourier transforms on the recorded data of the sample temperature and the heat-flow rate. The characteristic maximum of the heat-flow rate measured as a function of frequency is the result of the response to the temperature modulation which can be described as

$$A'_{\mathrm{T}}(\nu) = \frac{A_{\mathrm{T}}}{1 + (\nu\tau_{\mathrm{c}})^{\alpha}} \quad \text{and}$$

$$A''_{\mathrm{T}}(\nu) = \frac{(\nu\tau_{\mathrm{c}})^{\alpha/2} A_{\mathrm{T}}}{1 + (\nu\tau_{\mathrm{enthalpy}})^{\alpha}} \tag{5}$$

where A_{T} is the temperature amplitude at ν equal to zero. The measured temperature, T_{s}, is approximated by Eq. (5) when $\tau_{\mathrm{c}} = 36\,\mathrm{s}$, $A_{\mathrm{T}} = 0.45\,\mathrm{K}$, and $\alpha = 1.314$, as illustrated in Fig. 3 by the drawn line. Obviously, the reference temperature, T_{r}, behaves in the same manner with a set of different values of τ_{c}, A_{T}, α and can be calculated using the measured heat-flow rate which is proportional to $T_{\mathrm{r}} - T_{\mathrm{s}}$:

$$A_{\Phi}(\nu) = K\left[\frac{A_{\mathrm{Tr}}}{1 + (\nu\tau_{\mathrm{c_r}})^{\alpha_{\mathrm{r}}}} - \frac{A_{\mathrm{Ts}}}{1 + (\nu\tau_{\mathrm{c_s}})^{\alpha_{\mathrm{r}}}}\right] \tag{6}$$

where K is the experimentally found the Newton's law constant and subscripts r and s denote reference and sample, respectively. Having these functions, the sample and reference temperatures can be corrected to the frequency independent values, as is illustrated in Fig. 3 by the data for T_{s} corrected and T_{r} corrected [16].

2.4. Quasi-isothermal and standard LMDSC with an underlying rate of temperature change

The above procedure has been used to obtain the heat capacity of polystyrene as a function of frequency in the temperature range of the glass transition. The quasi-isothermal experiments were performed at the temperatures, T_0, which covered the range from the glass to the liquid, where the heat capacity is again frequency independent. The sample history was set by heating to 413 K followed by cooling to 343 K with a rate of $10\,\mathrm{K\,min^{-1}}$. The result of this experiment employing the multi-frequency modulation is illustrated in Fig. 4. Transformed to the temperature domain, these data are shown in Fig. 5. These figures should be compared to Figs. 1d and 2, to see the frequency extension relative to the TMDSC results.

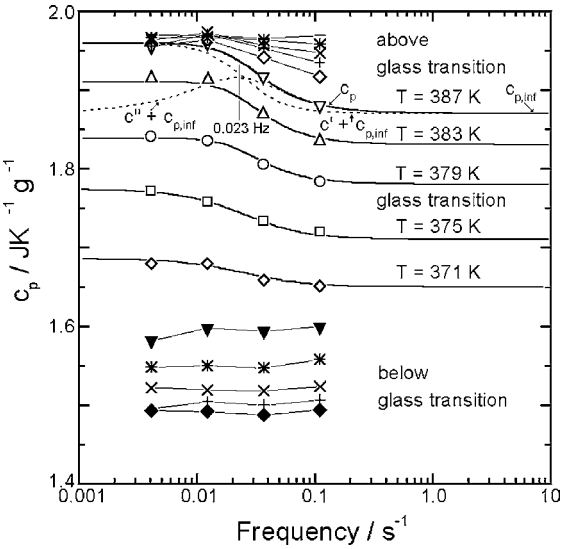

Fig. 4. Frequency-corrected specific heat capacities and their representation by Eqs. (4a) and (4b) in the region of the glass transition.

In addition, experiments with the light-modulation system using a single-frequency were carried out using an underlying rate of temperature change. In the first stage of the experiment, the sample was heated with a rate of $20\,\mathrm{K\,min^{-1}}$ to 413 K, above the glass transition, and kept there for more than 10 min with-

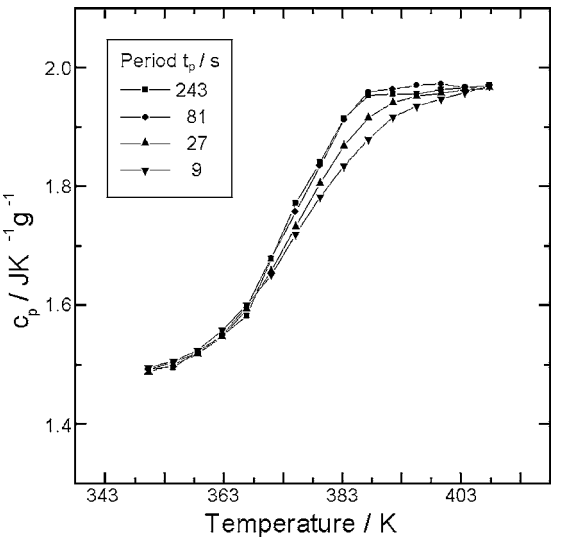

Fig. 5. Frequency-corrected heat capacities as a function of temperature for the periods indicated. Data from Fig. 4.

out data collection. Then the cooling and heating programs with underlying rates of $1\,\mathrm{K\,min^{-1}}$ were applied successively. During these runs data were collected continuously. The amplitude of the sample temperature by light-modulation of the sample, A_{Ts}, and the heat-flow rate A_{Φ} were calculated using the short-time-Fourier-transform (STFT) method [18], taking data from single, successive periods of modulation. The absolute value of the heat capacity was not the primary result in this experiment, and therefore no special procedure for frequency correction of the heat capacity was used. In this case the heat capacity was calculated from

$$mc_p = \frac{A_{\Phi}}{A_{\mathrm{Ts}}} \times K \tag{7}$$

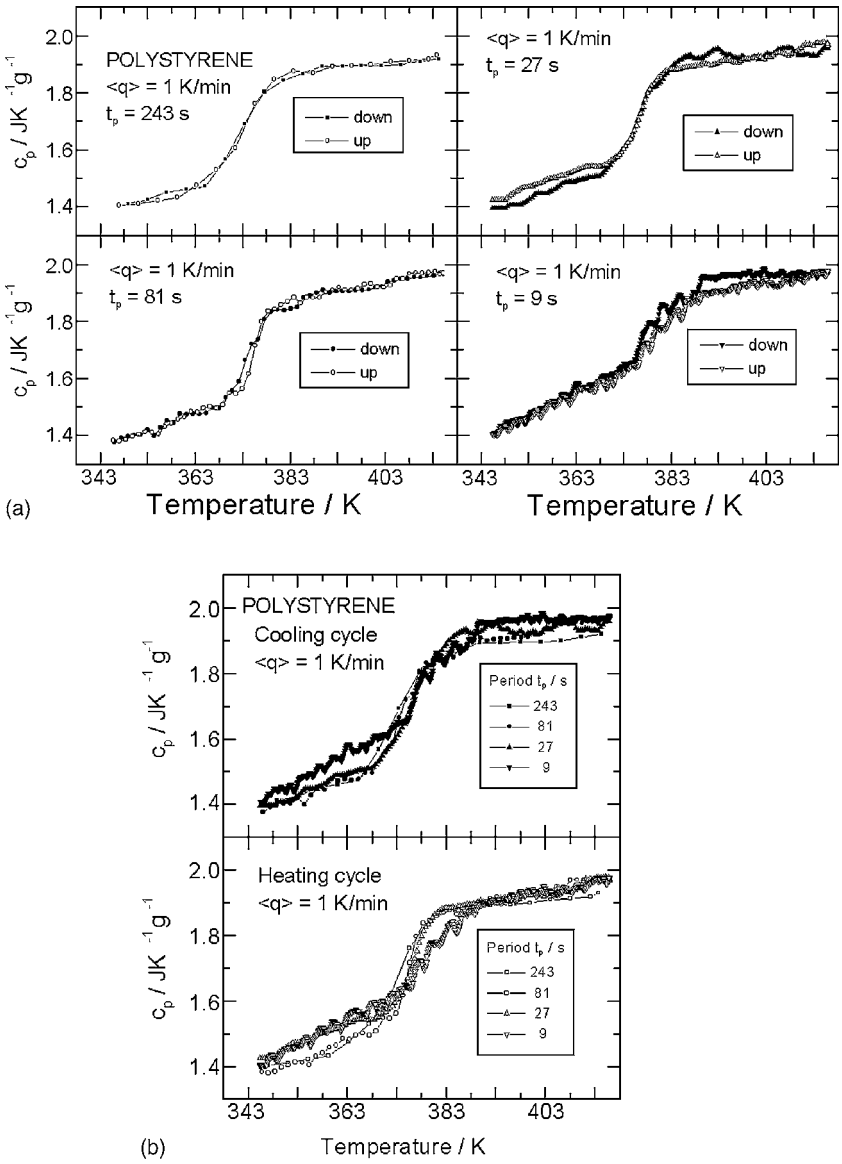

Fig. 6. (a) Glass transition of polystyrene obtained using underlying cooling and heating rates of $1\,\mathrm{K\,min^{-1}}$ for four different frequencies of LMDSC. (b) Glass transition for the cooling and heating cycles of (a) combined in single graphs.

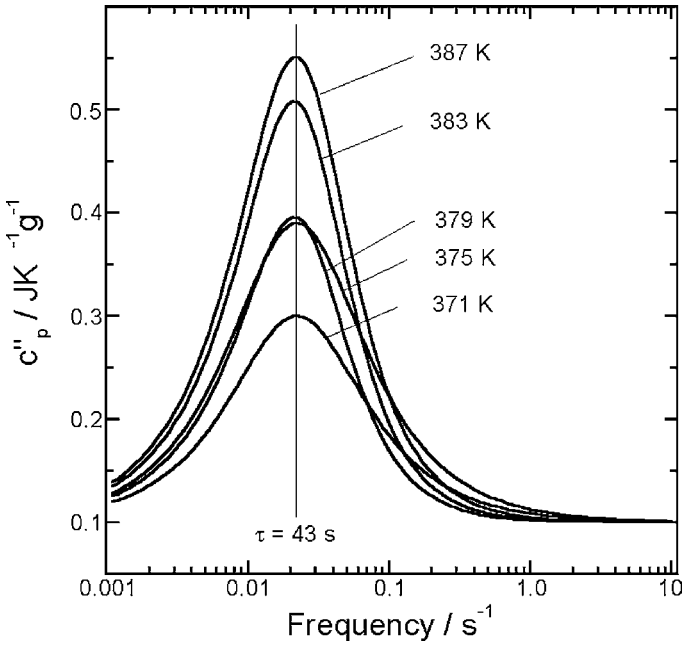

Fig. 7. Imaginary part of the specific heat capacity, c_p'', estimated from Eq. (4a).

where K is a correction factor for normalization of the heat capacity outside the glass transition to the values taken from the ATHAS data bank (Advanced Thermal Analysis System, for a description see, for example [19]). The result is illustrated in Fig. 6a where cooling/heating cycles are displayed for four separate frequencies. It is seen, that under these conditions the heat capacity in the region of the glass transition has the same character, independent of the direction of the temperature program. A small frequency dependency is seen when the data with different frequencies are selected from cooling and heating cycles and are compared, as done in Fig. 6b. These frequency dependencies of the heat capacities are less obvious in the frequency range of our experiments, but shows the same trends as discovered on comparing TMDSC data with different heating rates to quasi-isothermal TMDSC on heating and cooling [6].

3. Discussions and conclusions

From the presented experimental results it is seen, that the frequency-dependent heat capacity of polystyrene in the temperature region of the glass transition can be observed in a single complex sawtooth or multiple-frequency light-modulation at frequencies that may extend to higher values by a factor of about 10. The analysis is best carried out in the quasi-isothermal mode. The observations for multi-frequency sawtooth experiments are similar to those observed by single-frequency LMDSC. Noticeable is the fact, that when using a slow underlying change of temperature of $1\,\mathrm{K\,min^{-1}}$, the glass transition is largely independent on cooling and heating. The fast relaxation process, detected by multi-frequency DSC dependence on temperature, as is illustrated in Fig. 7. The imaginary part of Eq. (4a) is depicted for the approximations illustrated in Fig. 4. The time constant is estimated to be 43 s.

Acknowledgements

This work was supported by Division of Material Research, National Science Foundation, Polymers Program, Grant # DMR-9703692 and Division of Materials Sciences and Engineering, Office of Basic

Energy Sciences, US Department of Energy at Oak Ridge National Laboratory, managed and operated by UT-Batelle, LLC, for the US Department of Energy, under contract number DOE-AC05-00OR22725. Support for instrumentation came from TA Instrument, Inc.

References

[1] B. Wunderlich, D.M. Bodily, M.H. Kaplan, J. Appl. Phys. 35 (1964) 95.
[2] M. Reading, B.K. Hahn, B.S. Crowe, Method and Apparatus for Modulated Differential Analysis, US Patent 5 224 775 (6 July 1993).
[3] A. Boller, C. Schick, B. Wunderlich, Thermochim. Acta 266 (1995) 97.
[4] B. Wunderlich, A. Boller, I. Okazaki, S. Kreitmeier, J. Therm. Anal. 47 (1996) 1013.
[5] A. Boller, I. Okazaki, B. Wunderlich, Thermochim. Acta 284 (1996) 1.
[6] L.C. Thomas, A. Boller, I. Okazaki, B. Wunderlich, Thermochim. Acta 291 (1997) 85.
[7] I. Okazaki, B. Wunderlich, J. Polym. Sci. B 34 (1996) 2941.
[8] B. Wunderlich, I. Okazaki, J. Therm. Anal. 49 (1997) 57.
[9] B. Wunderlich, R. Androsch, M. Pyda, Y.K. Kwon, Thermochim. Acta 348 (2000) 181.
[10] P. Kamasa, M. Merzlyakov, M. Pyda, J. Pak, C. Schick, B. Wunderlich, Thermochim. Acta 392/393 (2002) 195.
[11] Y. Saruyama, Thermochim. Acta 304/305 (1997) 171.
[12] Y. Saruyama, Thermochim. Acta 330 (1999) 101.
[13] I. Moon, R. Androsch, B. Wunderlich, Thermochim. Acta 357/358 (2000) 285.
[14] B. Wunderlich, Y. Jin, A. Boller, Thermochim. Acta 238 (1994) 277.
[15] R. Androsch, I. Moon, S. Kreitmeier, B. Wunderlich, Thermochim. Acta 357/358 (2000) 267.
[16] P. Kamasa, A. Buzin, M. Pyda, B. Wunderlich, Thermochim. Acta 381 (2002) 139;
P. Kamasa, A. Buzin, M. Pyda, B. Wunderlich, in: K.J. Kociba, B.J. Kociba (Eds.), Proceedings of the 29th NATAS Conference, St. Louis, MO, September 24–26, 29, 2001, p. 323.
[17] M. Schwartz, Information Transmission, Modulation, and Noise, McGraw-Hill, Toronto, 1959.
[18] O. Rioul, M. Vetterli, IEEE Sig. Process. Mag. 8 (1991) 14.
[19] B. Wunderlich, Pure Appl. Chem. 67 (1995) 1991. For values see the downloadable database on the WWW [internet], URL: http://web.utk.edu/~athas.